Epsilon-near-zero behavior from plasmonic Dirac point: Theory and realization using two-dimensional materials

Marios Mattheakis,[1,2,*] Constantinos A. Valagiannopoulos,[3,†] and Efthimios Kaxiras[1,4]

[1]*School of Engineering and Applied Sciences, Harvard University, Cambridge, Massachusetts 02138, USA*

[2]*Crete Center for Quantum Complexity and Nanotechnology, Department of Physics, University of Crete, Heraklion 71003, Greece*

[3]*Department of Physics, Nazarbayev University, Astana 010000, Kazakhstan*

[4]*Department of Physics, Harvard University, Cambridge, Massachusetts 02138, USA*

The electromagnetic response of a two-dimensional metal embedded in a periodic array of a dielectric host can give rise to a plasmonic Dirac point that emulates epsilon-near-zero (ENZ) behavior. This theoretical result is extremely sensitive to structural features like periodicity of the dielectric medium and thickness imperfections. We propose that such a device can actually be realized by using graphene as the two-dimensional metal and materials like the layered semiconducting transition-metal dichalcogenides or hexagonal boron nitride as the dielectric host. We propose a systematic approach, in terms of design characteristics, for constructing metamaterials with linear, elliptical, and hyperbolic dispersion relations which produce ENZ behavior, normal or negative diffraction.

The confinement of metallic ("free") electrons in two-dimensional interfaces can produce powerful effects used to drive electromagnetic (EM) devices like nanoantennas with extremely short wavelength resonance [1,2], metalenses and optical holography [3–5], active plasmonic systems [6–8], and sub-wavelength Bloch oscillations [9,10]. The key feature for such applications is the creation of waves propagating along a metal-dielectric interface with wavelength shorter than that of the incident radiation, while the waves decay exponentially in the perpendicular direction. This surface effect involves electronic motion (plasmons) coupled with electromagnetic waves (polariton) and is referred to as surface plasmon polariton (SPP). By combining the properties of different materials, it is even possible to produce behavior not found under normal circumstances like negative refraction [11–16], epsilon-near-zero (ENZ) [17–19], discrete solitons [20,21], and quantum control of light [22,23].

The bottleneck in creating SPP devices with any desirable characteristic has been the limitations of typical three-dimensional solids in producing perfect interfaces for the confinement of electrons and the features of dielectric host. This may no longer be a critical issue. The advent of truly two-dimensional (2D) materials like graphene (a metal), transition-metal dichalcogenides (TMDC's, semiconductors), and hexagonal boron nitride (hBN, an insulator) make it possible to produce structures with atomic-level control of features in the direction perpendicular to the stacked layers [24–27]. This is ushering a new era in manipulating the properties of plasmons and designing devices with extraordinary behavior. In particular, 2D structures support plasmons (collective excitations) which fundamentally differ from SPPs, since the charge carriers are restricted in two dimensions [28,29]. Nevertheless, 2D plasmons and SPPs share similarities in field profiles and in dispersion behavior and could be used

interchangeably for the purposes of the present discussion. Plasmons in 2D materials exhibit ultra-sub-wavelength behavior [28–31]. Graphene is quite special, possessing exceptional optical properties due to its high quantum efficiency for light-matter interaction [29,32]. Doped graphene has been used as an effective plasmonic platform, since it supports both high- and low-energy plasmons due to inter- and intraband transitions [33].

ENZ metamaterials exhibit interesting properties like EM wave propagation with no phase delay [17]. As a consequence, the pattern of the transmitted/reflected waves can be tailored at will. Moreover, in a waveguide filled with ENZ medium, all the modes propagate irrespective of how small or thin the structure is, exhibiting supercoupling effects [18]. Much effort has been devoted toward the design of ENZ media [34]. Here, we propose a systematic method for constructing ENZ metamaterials by appropriate combination on 2D materials. We show analytically that multilayers of a plasmonic 2D material embedded in a dielectric host exhibit a plasmonic Dirac point (PDP), namely a point in wave-number space where two linear coexisting dispersion curves cross each other, which, in turn, leads to an effective ENZ behavior [35]. Specifically, EM wave propagation through layered heterostructures can be tuned dynamically by controlling the operating frequency and the doping level of the 2D metallic layers [13]. The presence of the PDP is extremely sensitive to structural features and can only be realized by truly 2D materials, due to the flatness on the atomic scale that 2D materials provide. To prove the feasibility of this design, we investigate numerically EM wave propagation in periodic plasmonic structures. They consist of 2D metallic layers lying on yz plane in the form of graphene arranged periodically along the x axis and possessing surface conductivity σ_s. The layers are embedded in a uniaxial dielectric host in the form of TMDC or hBN multilayers of thickness d and with nonlocal relative permittivity tensor $[\varepsilon_d]$ with diagonal components $\varepsilon_x \neq \varepsilon_y = \varepsilon_z$. We explore the resulting linear, elliptical, and hyperbolic EM dispersion relations which produce the ENZ effect, ordinary diffraction and negative diffraction, depending on the design features.

---

*mariosmat@seas.harvard.edu; http://scholar.harvard.edu/marios _matthaiakis/home

†konstantinos.valagiannopoulos@nu.edu.kz; https://sst.nu.edu.kz /konstantinos-valagiannopoulos/

We solve the analytical problem under transverse magnetic (TM) polarization, with the magnetic field parallel to the y direction, which implies that there is no interaction of the electric field with ε_y. We consider a lossless host, namely $\varepsilon_x, \varepsilon_z \in \mathbb{R}$, which is also magnetically inert (relative permeability $\mu = 1$). For monochromatic harmonic waves in time with TM polarization, $\mathbf{E} = (E_x, 0, E_z)$ and $\mathbf{H} = (0, H_y, 0)$, Maxwell equations lead to the three equations connecting the components of the $\mathbf{E}$ and $\mathbf{H}$ fields. For the longitudinal component [11,20], $E_z = (i\eta_0/k_0\varepsilon_z)(\partial H_y/\partial x)$ where $k_0 = \omega/c$ is the vacuum wave number at frequency ω and $\eta_0 = \sqrt{\mu_0/\varepsilon_0}$ is the free space impedance. Defining the vector of the transversal field components as $\mathbf{\Psi} = (E_x, H_y)^T$ gives [20]

$$i\frac{\partial}{\partial z}\mathbf{\Psi} = k_0\eta_0 \begin{pmatrix} 0 & 1 + \frac{1}{k_0^2}\frac{\partial}{\partial_x}\frac{1}{\varepsilon_z}\frac{\partial}{\partial_x} \\ \frac{\varepsilon_x}{\eta_0^2} & 0 \end{pmatrix}\mathbf{\Psi}. \quad (1)$$

For EM waves propagating along the z axis, namely $\mathbf{\Psi}(x,z) = \mathbf{\Psi}(x)e^{ik_z z}$, we obtain the eigenvalue problem for the wave number k_z of the SPPs along z [11,20]. The metallic 2D planes carry a surface current $J_s = \sigma_s E_z$, which acts as a boundary condition in the eigenvalue problem. The magnetic field must be $H_y^-(x)e^{ik_z z}$ for $-d < x < 0$ and $H_y^+(x)e^{ik_z z}$ for $0 < x < d$ on either side of the metallic plane at $x = 0$, with boundary conditions $H_y^+(0) - H_y^-(0) = \sigma_s E_z(0)$ and $\partial_x H_y^+(0) = \partial_x H_y^-(0)$. Using the Bloch character along x, due to the periodicity of the system, with Bloch wave number k_x: $H_y^+(x) = H_y^-(x - d)e^{ik_x d}$, we arrive at the dispersion relation [11]:

$$F(k_x, k_z) = \cos(k_x d) - \cosh(\kappa d) + \frac{\xi\kappa}{2}\sinh(\kappa d) = 0, \quad (2)$$

where $\kappa^2 = (\varepsilon_z/\varepsilon_x)(k_z^2 - k_0^2\varepsilon_x)$ expresses the anisotropy of the host medium and $\xi = -(i\sigma_s\eta_0/k_0\varepsilon_z)$ is the "plasmonic thickness" which determines the SPP decay length [11,31]. For lossless 2D metallic planes, σ_s is purely imaginary and ξ is purely real (from the assumption of $\varepsilon_z \in \mathbb{R}$). At the center of the first Brillouin zone $k_x = 0$, the equation has a trivial solution [11] for $\kappa = 0 \Rightarrow k_z = k_0\sqrt{\varepsilon_x}$ which corresponds to propagation of x-polarized fields travelling into the host medium with refractive index $\sqrt{\varepsilon_x}$ without interacting with the 2D planes which are positioned along the z axis [15]. Near the Brillouin zone center ($k_x/k_0 \ll 1$ and $\kappa \simeq 0$) and under the reasonable assumption of a very dense grid ($d \to 0$), we obtain $k_x d \ll 1$ and $\kappa d \ll 1$, and we Taylor expand Eq. (2) to second order in d:

$$\frac{k_z^2}{\varepsilon_x} + \frac{d}{(d-\xi)\varepsilon_z}k_x^2 = k_0^2. \quad (3)$$

From a metamaterial point of view [13,14], the entire system is treated as a homogeneous anisotropic medium with effective relative permittivities given by

$$\varepsilon_x^{\text{eff}} = \varepsilon_x, \quad \varepsilon_z^{\text{eff}} = \varepsilon_z + i\frac{\eta_0\sigma_s}{k_0 d} = \varepsilon_z\frac{d-\xi}{d}. \quad (4)$$

The approximate dispersion relation Eq. (3) is identical to that of an equivalent homogenized medium described by Eq. (4): $k_z^2/\varepsilon_x^{\text{eff}} + k_x^2/\varepsilon_z^{\text{eff}} = k_0^2$. Indeed, a very dense mesh of 2D media is a prerequisite for homogenization [30,36,37]. Equation (4) indicates the capability to control the behavior of the overall structure along the z direction: The choice $d = \varepsilon_z/(\varepsilon_z - \varepsilon_x)\xi$

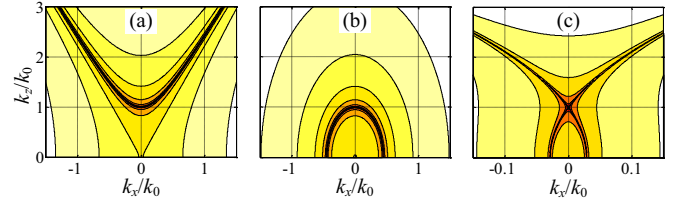FIG. 1. Magnitude of the function $\log|F(k_x, k_z)|$ (darker to lighter colors = smaller to larger values); $F(k_x, k_z) = 0$ corresponds to black. (a) $d < \xi$, strong SPP coupling; (b) $d > \xi$, weak SPP coupling; (c) $d = \xi$, plasmonic Dirac point.

leads to an isotropic effective medium, $\varepsilon_z^{\text{eff}} = \varepsilon_x^{\text{eff}}$. For the lossless case, $\xi \in \mathbb{R}$, we identify three possibilities, provided an ordinary material ($\varepsilon_x, \varepsilon_z > 0$) is used as host:

(i) $\xi > d$, strong SPP coupling: SPPs develop along the z direction at the interface between the conducting planes and the dielectric host. In this case, the overall effective response of the system becomes also plasmonic, with Bloch plasmon polaritons waves [37] created along the x direction. The shape of the supported band on the (k_x, k_z) plane is hyperbolic, since the system behaves as a hyperbolic metamaterial [11,15,36] with $\varepsilon_z^{\text{eff}} < 0$, $\varepsilon_x^{\text{eff}} > 0$, Fig. 1(a).

(ii) $0 < \xi < d$, weak SPP coupling: Since ξ is still positive, SPPs develop along the z direction between the conducting plane and the dielectric host. However, the effective behavior of the entire structure is not dominated by SPP coupling [11] and the shape of the dispersion relation on the (k_x, k_z) plane is an ellipse since $\varepsilon_z^{\text{eff}}, \varepsilon_x^{\text{eff}} > 0$, Fig. 1(b).

(iii) $\xi < 0$: In this case, the 2D planes do not support plasmonic modes. The dispersion relation on the (k_x, k_z) plane is an ellipse, as in an ordinary photonic crystal [12,36], with $\varepsilon_z^{\text{eff}}, \varepsilon_x^{\text{eff}} > 0$, Fig. 1(b).

When either the 2D medium ($\text{Re}[\sigma_s] \neq 0$) or the host material ($\text{Im}[\varepsilon_z] \neq 0$) are lossy, a similar separation holds by replacing ξ by $\text{Re}[\xi]$.

The most interesting case is the linear dispersion, where k_z is linearly dependent on k_x and dk_x/dk_z is constant for a wide range of k_z [11,36]. When this condition holds, the spatial harmonics travel with the same group velocity into the effective medium [11,12]. To engineer our structure to exhibit a close-to-linear dispersion relation, we inspect the approximate version of Eq. (3): A huge coefficient for k_x will make k_0^2 on the right-hand side insignificant; if $\xi = d$, the term proportional to k_x^2 increases without bound yielding a linear relation between k_z and k_x. With this choice, $\sigma_s = -i(k_0 d\varepsilon_z/\eta_0)$, and substituting in the exact dispersion relation Eq. (2), we find that $(k_x, k_z) = (0, k_0\sqrt{\varepsilon_x})$ becomes a saddle point for the transcendental function $F(k_x, k_z)$ giving rise to the conditions for the appearance of two permitted bands, namely two lines on the (k_x, k_z) plane across which $F(k_x, k_z) = 0$. This argument connects a mathematical feature, the saddle point of the dispersion relation, with a physical feature, the crossing point of the two coexisting linear dispersion curves, the plasmonic Dirac point [35], as indicated in Fig. 1(c). From a macroscopic point of view, the choice $\xi = d$ makes the effective permittivity along the z direction vanish, as is evident from Eq. (4). The existence of a PDP makes the

effective medium behave like an ENZ material in one direction ($\varepsilon_z^{\text{eff}} = 0$).

The very special behavior associated with the PDP would be of restricted usefulness if its existence were sensitively depended on the the exact fulfillment of the condition $\text{Re}[\xi] = d$, where losses have been taken into account ($\text{Im}[\xi] \neq 0$). For this reason, we investigate the behavior of the gap created between the two bands on the (k_x, k_z) plane, when the PDP breaks down. At the center of the Brillouin zone ($k_x = 0$), where the minimum gap is created [35–37], the dispersion relation Eq. (2) is $g(k_z) = 2[\cosh(\kappa d) - 1]/[\kappa \sinh(\kappa d)] = \xi$. Near the PDP, $k_z = k_0\sqrt{\varepsilon_x} + \Delta k_z$ and $\xi = d + \Delta\xi$, while $g(k_z) \cong g(k_0\sqrt{\varepsilon_x}) + g'(k_0\sqrt{\varepsilon_x})\Delta k_z$; given that $g(k_z) = d$ and $g'(k_z) = -(k_0 d^3 \varepsilon_z / 6\sqrt{\varepsilon_x})$ in the limit $k_z \to k_0\sqrt{\varepsilon_x}$, a direct relation between Δk_z and $\Delta\xi$ is obtained,

$$\frac{\Delta k_z}{k_0\sqrt{\varepsilon_x}} = -\frac{6}{(k_0 d)^2 \varepsilon_z} \frac{\Delta\xi}{d}. \tag{5}$$

In the derivation of Eq. (5), we assume that $\Delta\xi$ is small compared to d in the vicinity of the PDP, that is, $d = \text{Re}[\xi]$, leading to two conditions: $\text{Re}[\Delta\xi]/d \ll 1$ and $\text{Im}[\Delta\xi]/d \ll 1$. Near the PDP the former condition is satisfied, since $\text{Re}[\Delta\xi] = \text{Re}[\xi] - d \to 0$. For the imaginary part we have, $\text{Im}[\Delta\xi]/d = \text{Im}[\xi]/\text{Re}[\xi] = \text{Re}[\sigma_s]/\text{Im}[\sigma_s] \ll 1$, which is satisfied if the system is characterized by low losses. To illustrate the situation with an example, we use the Drude model to describe the conductivity of a 2D metal, as is appropriate for doped graphene. In this case $\text{Re}[\sigma_s]/\text{Im}[\sigma_s] = 1/\tau\omega$, where τ accounts for losses. For representative values of τ and ω, we obtain $1/(\tau\omega) \simeq 10^{-2}$, which makes our assumption of low losses reasonable. Moreover, in Eq. (5) the real and imaginary parts have been decoupled, that is, the losses, corresponding to $\text{Im}[\Delta\xi]$, do not affect the band gap given by $\text{Re}[\Delta k_z]$.

The choice $k_z = k_0\sqrt{\varepsilon_x}$ works as a trivial solution of the dispersion equation regardless of the values of the rest of the parameters. Consequently, in the vicinity of $\xi = d$, Eq. (5) gives the relative spread of the gap ($\Delta k_z/k_0\sqrt{\varepsilon_x}$) between the two bands since it implies that $k_z = k_0\sqrt{\varepsilon_x} + \Delta k_z$ is also a solution of Eq. (2) at $k_x = 0$. Since the lattice of the 2D medium is electrically dense ($k_0 d \ll 1$), Eq. (5) indicates a substantial sensitivity of the PDP on the value of $\Delta\xi$. As a consequence, a small error on the $\xi = d$ condition leads to a significant gap between the two bands: Taking an isotropic silica glass with $\varepsilon_x = \varepsilon_z = 4$ as host material, a deviation of order ($\Delta\xi/d) \cong$ 10% gives rise to a band gap of order $\Delta k_z \cong 10^3 k_0$ for $k_0 d = 10^{-2}$. It should be additionally stressed that only one band moves from the PDP position: For $\Delta\xi < 0 \Rightarrow \xi < d$ the upper point of the elliptical band remains at $(k_x, k_z) = (0, k_0\sqrt{\varepsilon_x})$, whereas the hyperbolic band moves to higher values of k_z at a rate given by Eq. (5) with the converse behavior for $\Delta\xi > 0 \Rightarrow \xi > d$.

The extreme sensitivity of the PDP on the spatial period d between the 2D planes makes the use of regular materials as dielectric hosts impractical, unless the dielectric host is also a 2D material with atomic scale control of the thickness d and no roughness. For instance, one could build the dielectric host by stacking 2D layers of materials like hBN [23,24] or molybdenum disulfide (MoS$_2$) [25–27] with essentially perfect planarity, complementing the planarity of graphene, which has been used extensively in optoelectronic and
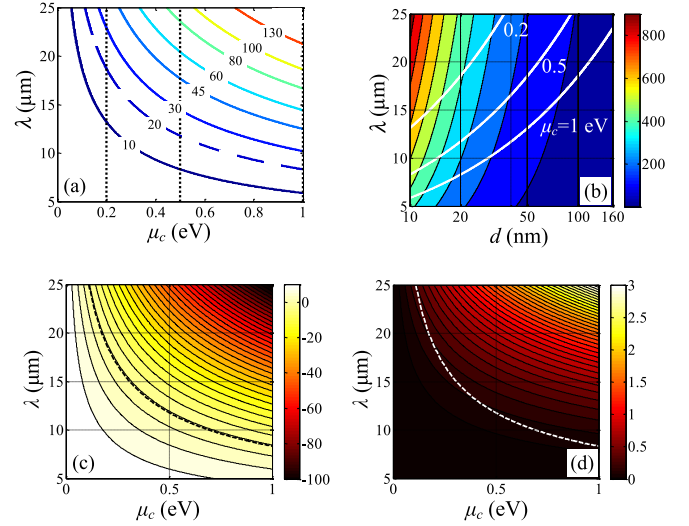

FIG. 2. (a) Combinations of graphene chemical potential μ_c and free space operational wavelengths λ leading to ENZ behavior (PDP in dispersion relation) for several lattice periods d (in nm). (b) The propagation distance L of a plasmonic mode in units of d for all the combinations of the wavelength λ and the period d leading to ENZ effect. The white lines show representative levels of graphene doping [dotted lines in (a)]. (c) Real (d) imaginary parts of the effective permittivity $\varepsilon_z^{\text{eff}}$ of the effective medium for the choice $d = 20$ nm [dashed line in (a)]; dashed curves indicate the ENZ regime.

plasmonic applications [29]. The surface conductivity σ_s of an infinite graphene plane includes both intraband and interband transition contributions [33], with the intraband contribution dominating at THz frequencies which is approximated by the Drude model, $\sigma_s(\omega) = ie^2\mu_c/[\pi\hbar^2(\omega + i/\tau)]$, where μ_c is the tunable chemical potential and τ is the transport scattering time of the electrons [4,11,29,36]. In the following, we use bulk MoS$_2$, which at THz frequencies is assumed lossless with a diagonal permittivity tensor of elements, $\varepsilon_x \cong 3.5$ (out of plane) and $\varepsilon_y = \varepsilon_z \cong 13$ (in plane) [25–27]. The optical losses of graphene are taken into account using $\tau = 0.5$ ps [11]. In Fig. 2(a), we show the combinations of μ_c and the operational wavelength in free space λ which lead to a PDP for several values of lattice density distances $d = \text{Re}[\xi]$ in nm.

The ENZ behavior should be accompanied by low effective losses, otherwise the propagating field is damped fast. A crucial quantity demonstrating the efficiency of the proposed medium is the length L that an EM wave can propagate into such a device without losing a significant part of its power. We find that the length L before the amplitude falls to the $1/e$ of its maximal value, in units of the period d, is given by:

$$\frac{L}{d} = \sqrt{\frac{2}{\varepsilon_z}} \sqrt{\frac{\text{Im}[\sigma_s]}{\text{Re}[\sigma_s]}} \frac{1}{k_0 d}. \tag{6}$$

From Eq. (6), the propagating beam travels along x for more lattice periods, the less lossy the graphene sheets and the denser the lattice. The seeming contradiction of longer propagation in a denser lattice can be explained by the stronger SPP coupling for smaller periods d [11]. Using the Drude model for σ_s gives $L/d = \sqrt{c\tau\lambda}/(d\sqrt{\varepsilon_z}\pi)$. This is shown in Fig. 2(b) by a contour plot as a function of free-space wavelength λ and

cell physical size d and takes values in the range of several hundreds. The loss-unaffected transmission length in terms of the number of wavelength cannot be determined explicitly by Eq. (6), because σ_s depends on λ. Nevertheless, an explicit expression of L in terms of the number of wavelengths λ can be calculated, in the context of the Drude model. Equation (6) can be rewritten as $L/\lambda = \sqrt{c\tau/(\varepsilon_z \pi \lambda)}$, indicating that L/λ is inversely proportional to $\sqrt{\lambda}$ and has no dependence on the doping level μ_c. The proposed design exhibits no significant losses of the propagating wave even in long structures consisting of several hundred periods. Interestingly, the best results (smallest losses) do not require large graphene doping.

To illustrate, for a reasonable distance between successive graphene planes of $d = 20$ nm, the real [Fig. 2(c)] and imaginary [Fig. 2(d)] permittivity values that can be emulated by this specific graphene-MoS$_2$ architecture determine the device characteristics at different frequencies (λ) and graphene doping levels (μ_c). Positive values of Re[$\varepsilon_z^{\text{eff}}$] are relatively moderate and occur for larger frequencies and lower doping levels of graphene; on the other hand, Im[$\varepsilon_z^{\text{eff}}$] is relatively small in the ENZ region as indicated by a dashed line in both graphs. Such a fact renders our theoretical assumptions for lossless structures quite realistic; however, losses become larger as Re[$\varepsilon_z^{\text{eff}}$] gets more negative. As these results show, the extreme sensitivity of the PDP on d can be turned into an advantage for device fabrication: The proper combination of d and μ_c can be selected to produce a device that operates at a given frequency (λ), as the practical limitations of layer stacking (d) or graphene doping (μ_c) dictate.

To examine the actual EM field distribution in our graphene-MoS$_2$ configuration for each of the three characteristic cases of supported bands, we excite a finite structure consisting of 40 graphene planes and Re[ξ] = 20.8 nm for operational wavelength in vacuum $\lambda = 12$ μm, using as a source a 2D magnetic dipole positioned close to one of its two interfaces and oriented parallel to them; this choice of source allows us to study the system's response when exciting all the incidence angles with the same power. The spatial distribution of the magnetic field value is shown in Fig. 3 where the volume containing the graphene multilayers is denoted by a thick black frame. In all three cases, the reflections are negligible because the background region is filled with a medium of the same dielectric properties as MoS$_2$. In Fig. 3(a), the system is in the critical case ($d = $ Re[ξ]), where the wave propagates through the
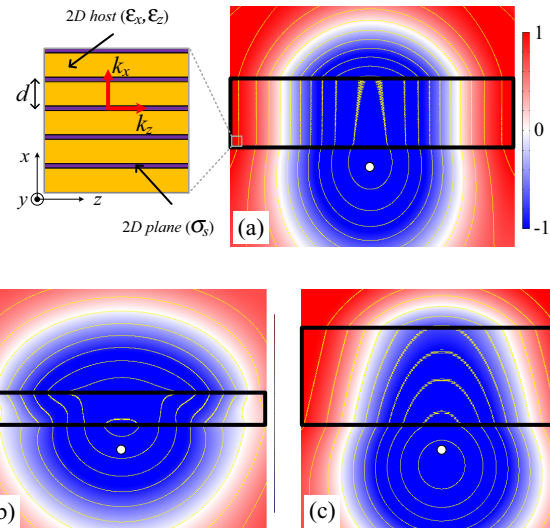

FIG. 3. Spatial distribution of the axial magnetic field of a device consisting of 40 graphene sheets embedded in MoS$_2$ background excited by a magnetic dipole at the point marked as white dot. The thick black boundary defines the volume containing the graphene multilayers. (a) $d = $ Re[ξ] (ENZ behavior); the inset has details of the graphene multilayer configuration. (b) $d = 0.5$Re[ξ] (hyperbolic metamaterial). (c) $d = 1.5$Re[ξ] (elliptical medium). Re[ξ] = 20.8 nm.

graphene sheets without dispersion as in an ENZ medium. In Fig. 3(b), the interlayer distance is $d = 0.5$Re[ξ] (strong SPP coupling regime) and the system shows negative (anomalous) diffraction with the front of the propagating wave into the multilayered structure showing a hyperbolic shape. In Fig. 3(c), $d = 1.5$Re[ξ] (weak SPP coupling regime) and the EM wave shows ordinary diffraction through the graphene planes.

[1] W. L. Barnes, A. Dereux, and T. W. Ebbesen, Nature **424**, 824 (2003).

[2] J. Dorfmüller, R. Vogelgesang, W. Khunsin, C. Rockstuhl, C. Etrich, and K. Kern, Nano Lett. **10**, 3596 (2010).

[3] L. Huang *et al.*, Nat. Commun. **4**, 2808 (2013).

[4] J. Cheng, W. Li Wang, H. Mosallaei, and E. Kaxiras, Nano Lett. **14**, 50 (2014).

[5] D. Wintz, P. Genevet, A. Ambrosio, A. Woolf, and F. Capasso, Nano Lett. **15**, 3585 (2015).

[6] H. Alaeian and J. A. Dionne, Phys. Rev. A **89**, 033829 (2014).

[7] M. Mattheakis, T. Oikonomou, M. I. Molina, and G. P. Tsironis, IEEE J. Sel. Top. Quantum Electron. **22**, 5000206 (2016).

[8] C. A. Valagiannopoulos, IEEE J. Sel. Top. Quantum Electron. **22**, 89 (2016).

[9] T. Sfez *et al.*, J. Opt. Soc. Am. B **27**, 1617 (2010).

[10] A. Block, C. Etrich, T. Limboeck, F. Bleckmann, E. Soergel, C. Rockstuhl, and S. Linden, Nature Comm. **5**, 3843 (2014).

[11] B. Wang, X. Zhang, F. J. García-Vidal, X. Yuan, and J. Teng, Phys. Rev. Lett. **109**, 073901 (2012).

[12] Y. Liu and X. Zhang, Appl. Phys. Lett. **103**, 141101 (2013).

[13] I. V. Iorsh, I. S. Mukhin, I. V. Shadrivov, P. A. Belov, and Y. S. Kivshar, Phys. Rev. B **87**, 075416 (2013).

[14] C. A. Valagiannopoulos and S. A. Tretyakov, New J. Phys. **16**, 063004 (2014).

[15] C. A. Valagiannopoulos, M. S. Mirmoosa, I. S. Nefedov, S. A. Tretyakov, and C. R. Simovski, J. Appl. Phys. **116**, 163106 (2014).

[16] A. A. High, R. C. Devlin, A. Dibos, M. Polking, D. S. Wild, J. Perczel, N. P. de Leon, M. D. Lukin, and H. Park, Nature **522**, 192 (2015).

[17] A. Alù, M. G. Silveirinha, A. Salandrino, and N. Engheta, Phys. Rev. B **75**, 155410 (2007).

[18] M. Silveirinha and N. Engheta, Phys. Rev. Lett. **97**, 157403 (2006).

[19] M. A. K. Othman, C. Guclu, and F. Capolino, J. Nanophoton. **7**, 073089 (2013).

[20] Y. Liu, G. Bartal, D. A. Genov, and X. Zhang, Phys. Rev. Lett. **99**, 153901 (2007).

[21] Y. V. Bludov, D. A. Smirnova, Y. S. Kivshar, N. M. R. Peres, and M. I. Vasilevskiy, Phys. Rev. B **91**, 045424 (2015).

[22] M. S. Tame, K. R. McEnery, S. K. Özdemir, J. Lee, S. A. Maier, and M. S. Kim, Nat. Phys. **9**, 329 (2013).

[23] S. Dai *et al.*, Nat. NanoTech. **10**, 682 (2015).

[24] K. K. Kim, A. Hsu, X. Jia, S. M. Kim, Y. Shi, M. Dresselhaus, T. Palacios, and J. Kong, ACS Nano **6**, 8583 (2012).

[25] E. J. G. Santos and E. Kaxiras, ACS Nano **7**, 10741 (2013).

[26] X. Chen *et al.*, Nat. Commun. **6**, 6088 (2015).

[27] R. K. Defo, S. Fang, S. N. Shirodkar, G. A. Tritsaris, A. Dimoulas, and E. Kaxiras, Phys. Rev. B **94**, 155310 (2016).

[28] M. Jablan, H. Buljan, and M. Soljaččić, Phys. Rev. B **80**, 245435 (2009).

[29] A. N. Grigorenko, M. Polini, and K. S. Novoselov, Nat. Photon. **6**, 749 (2012).

[30] R. L. Chern and D. Han, Opt. Express **22**, 4817 (2014).

[31] B. Wang, X. Zhang, K. P. Loh, and J. Teng, J. Appl. Phys. **115**, 213102 (2014).

[32] Z. Fei *et al.*, Nature **487**, 82 (2012).

[33] Y. V. Bludov, A. Ferreira, N. M. R. Peres, and M. I. Vasilevskiy, Int. J. Mod. Phys. B. **27**, 1341001 (2013).

[34] E. Forati and G. W. Hanson, New J. Phys. **15**, 123027 (2013)

[35] H. Deng, F. Ye, B. A. Malomed, X. Chen, and N. C. Panoiu, Phys. Rev. B **91**, 201402(R) (2015).

[36] A. A. Orlov, S. V. Zhukovsky, I. V. Iorsh, and P. A. Belov, Photon. Nanostruct. Fundam. Appl. **12**, 213 (2014).

[37] S. V. Zhukovsky, A. Andryieuski, J. E. Sipe, and A. V. Lavrinenko, Phys. Rev. B **90**, 155429 (2014).